

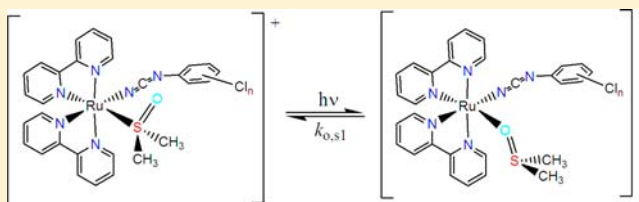
Phenylcyanamide Ligand Control of Photo-Induced Linkage Isomerism

Mohammad M. R. Choudhuri and Robert J. Crutchley*

Chemistry Department, Carleton University, Ottawa, Ontario K1S 5B6, Canada

S Supporting Information

ABSTRACT: The photo- and electrochemically induced linkage isomerism of six new complexes $[\text{Ru}(\text{bpy})_2(\text{L})(\text{dmsO-S})]^+$, where dmsO is dimethylsulfoxide, bpy is 2,2'-bipyridine, and L^- is pentachloro-, 2,3,5,6-tetrachloro-, 2,4,5-trichloro-, 2,4-dichloro-, 4-chloro-, and unsubstituted phenylcyanamide anion, were investigated. The quantum yields of linkage isomerism forming the metastable $[\text{Ru}(\text{bpy})_2(\text{L})(\text{dmsO-O})]^+$ complexes are shown to decrease with increasing donor properties of the phenylcyanamide ligand, and it is suggested that the donor properties of the cyanamide ligand stabilize the $[\text{Ru}(\text{bpy})_2(\text{L})(\text{dmsO-S})]^+$ complexes in the $^3\text{MLCT}$ excited state. The cyclic voltammetry of these complexes showed two oxidation processes: a phenylcyanamide $\text{L}(0/-)$ couple (an assignment supported by density functional theory (DFT) calculations) and a $\text{Ru}(\text{III}/\text{II})$ couple at more positive potential. Upon oxidation to $\text{Ru}(\text{III})$, the complexes rearranged to form $\text{Ru}-\text{O}$ linkage isomers, and the scan rate dependent voltammograms permitted estimates of the rates of linkage isomerism.



INTRODUCTION

Photochromism has been a field of intense study because of its application to optical memory¹ and photoswitching devices.² In this regard, dimethylsulfoxide (dmsO) in $[\text{Ru}(\text{tpy})(\text{bpy})(\text{dmsO-S})]^{2+}$, where tpy is 2,2':6',2''-terpyridine and bpy is 2,2'-bipyridine, has been shown to undergo rapid photoinduced linkage isomerism $\text{Ru}-\text{S} \rightarrow \text{Ru}-\text{O}$ followed by a far slower thermal $\text{Ru}-\text{O} \rightarrow \text{Ru}-\text{S}$ reaction in solution, crystals and films.³ The excited state responsible for this rearrangement arises from a metal-to-ligand charge transfer (MLCT) transition, and it is therefore not surprising that the electrochemical oxidation of $\text{Ru}(\text{II})$ to $\text{Ru}(\text{III})$ induces the same rearrangement with $\text{Ru}(\text{II})-\text{S}$ and $\text{Ru}(\text{III})-\text{O}$ being the stable bonding modes of dmsO.⁴ Since these earlier publications, ultrafast transient absorption studies of ruthenium(II) dmsO complexes⁵ have revealed that photoinduced linkage isomerism occurs in the picosecond time scale from a previously populated $^3\text{MLCT}$ excited state and, in the case of chelating sulfoxide complexes, linkage isomerism was observed on the femtosecond time scale.⁴⁰

In past studies, metal–metal coupling in dinuclear ruthenium complexes bridged by aromatic cyanamide ligands has been shown to be sensitive to the nature of the inner coordination sphere and the solvent.⁶ If these changes in metal–metal coupling could be induced photochemically, it would have significant photonics applications particularly in the case of mixed-valence complexes that possess intense intervalence bands which overlap the low-loss region of optical fibers in the NIR region. This is because transmission in the NIR region could be turned on/off by the changing energy and intensity of intervalence bands with the magnitude of metal–metal coupling. However, before one can create a “photo-switch”

mixed-valence complex, it is first necessary to find a mononuclear coordination environment that has the potential in a dinuclear complex to simultaneously express both properties of photoisomerism and mixed-valency. Toward this end, we now report the photo- and electrochemically induced linkage isomerism of six new complexes $[\text{Ru}(\text{bpy})_2(\text{L})(\text{dmsO-S})]^+$, where L^- is pentachloro- (Cl_5pcyd^-), 2,3,5,6-tetrachloro- (Cl_4pcyd^-), 2,4,5-trichloro- (Cl_3pcyd^-), 2,4-dichloro- (Cl_2pcyd^-), 4-chloro- (Clpcyd^-), and unsubstituted (pcyd^-) phenylcyanamide. For these complexes, the photoinduced linkage isomerism of dmsO is shown to be remarkably sensitive to the nature of the phenylcyanamide ligand.

EXPERIMENTAL SECTION

Materials. Ammonium hexafluorophosphate (99.5%, Alfa Aesar), ruthenium trichloride hydrate (99.9%, Alfa Aesar), 2,2'-bipyridine (Reagent plus, $\geq 99\%$, Sigma-Aldrich), dimethyl sulfoxide (anhydrous, $\geq 99.5\%$, Sigma-Aldrich), and dimethylformamide DMF (Caledon) were used as received. The ligands LH = phenylcyanamide (pcydH), 4-chloro- (ClpcydH), 2,4-dichloro- (Cl_2pcydH), 2,4,5-trichloro- (Cl_3pcydH), 2,3,5,6-tetrachloro- (Cl_4pcydH), pentachloro-phenylcyanamide (Cl_5pcydH), and their corresponding thallium salts, and reagent *cis*- $\text{Ru}(\text{bpy})_2(\text{L})_2$ complexes were prepared by following literature methods.⁷

Complex Syntheses. *Preparation of $[\text{Ru}(\text{bpy})_2(\text{pcyd})(\text{dmsO-S})][\text{PF}_6] \cdot 1.5\text{H}_2\text{O}$.* A mixture of *cis*- $\text{Ru}(\text{bpy})_2(\text{pcyd})_2$ (0.72 g, 1.11 mmol) and NH_4PF_6 (0.18 g, 1.12 mmol) in dmsO (20 mL) was refluxed under inert atmosphere for 20 min during which time the reaction solution color changed from purple to yellow-orange. The volume of the solution was then reduced under vacuum at temperature of $\sim 100^\circ\text{C}$ to almost dryness (prolonged heating may result in some

Received: October 15, 2013

Published: November 27, 2013

bis-dmsO byproduct). The residue was dissolved in 10 mL of acetone, filtered, and to the filtrate was added 200 mL of diethyl ether, precipitating the yellow-orange product. Yield: 0.80 g, 89%. Anal. Calcd. for $C_{29}H_{30}N_6PF_6RuSO_{2.5}$: C, 44.62; H, 3.87; N, 10.76. Found: C, 44.70; H, 3.54; N, 10.84. 1H NMR in ppm (300 MHz, dmsO- d_6): 10.04 (d, 1H), 9.17 (d, 1H), 8.88 (d, 1H), 8.82 (d, 1H), 8.77 (d, 1H), 8.72 (d, 1H), 8.44 (t, 1H), 8.32 (t, 1H), 8.16 (t, 1H), 8.07 (t, 1H), 8.03–7.92 (m, 1H), 7.90 (d, 1H), 7.51 (t, 1H), 7.43 (t, 1H), 7.23 (d, 1H), 6.85 (t, 1H), 6.49 (t, 1H), 6.11 (d, 1H), 3.19 (s, 3H), 2.22 (s, 3H). IR (KBr): $\nu(NCN)$, 2175 and 2147; $\nu(S=O)$, 1092 cm^{-1} .

Preparation of $[Ru(bpy)_2(Cl_3pcyd)(dmsO-S)]PF_6 \cdot H_2O$. This complex was prepared by following the same procedure as above with modification. A mixture of *cis*-Ru(bpy) $_2$ (Cl $_3$ pcyd) $_2$ (0.80 g, 1.12 mmol) and NH $_4$ PF $_6$ (0.18 g, 1.12 mmol) in 20 mL of dmsO was refluxed under argon for 1 h. The volume of the reaction solution was reduced as described above and after dissolving the residue in acetone and precipitation with diethyl ether gave 0.8 g of crude product. This was purified by chromatography through an alumina column (350 g, grade V) using CH $_2$ Cl $_2$ and acetone as eluents. The second dark-brown band containing the desired product was eluted with 100% acetone. After removal of the solvent, the dry solid was digested in 15 mL of acetonitrile and filtered. The dark-brown filtrate was reduced using a rotavap, and the residue redissolved in 10 mL of acetone. The addition of 200 mL of diethyl ether to this acetone solution precipitated the dark-orange product which was filtered and vacuum-dried. Yield: 0.30 g, 35%. Anal. Calcd. for $C_{29}H_{28}N_6Cl_3PF_6RuSO_2$: C, 43.21; H, 3.50; N, 10.43. Found: C, 43.13; H, 3.18; N, 10.41. 1H NMR in ppm (300 MHz, dmsO- d_6): 10.02 (d, 1H), 9.14 (d, 1H), 8.88 (d, 1H), 8.83 (d, 1H), 8.78 (d, 1H), 8.72 (d, 1H), 8.43 (t, 1H), 8.34 (t, 1H), 8.16 (t, 1H), 8.08 (t, 1H), 8.03–7.92 (m, 2H), 7.90 (d, 1H), 7.51 (t, 1H), 7.44 (t, 1H), 7.23 (d, 1H), 6.86 (d, 2H), 6.07 (d, 2H), 3.18 (s, 3H), 2.23 (s, 3H). IR (KBr): $\nu(NCN)$, 2171 and 2142; $\nu(S=O)$ 1090 cm^{-1} .

Preparation of $[Ru(bpy)_2(Cl_2pcyd)(dmsO-S)]PF_6$. This complex was prepared by following the same procedure as above with some modification. A mixture of *cis*-Ru(bpy) $_2$ (Cl $_2$ pcyd) $_2$ (1.16 g, 1.48 mmol) and NH $_4$ PF $_6$ (0.25 g, 1.53 mmol) was refluxed in 20 mL of dmsO under argon for 30 min. The volume of the reaction solution was reduced as described above and after dissolving the residue in acetone and precipitation with diethyl ether gave 1.18 g of crude product. A portion (0.65 g) of the crude product was purified by chromatography through an alumina column (400 g, grade V) using CH $_2$ Cl $_2$, acetone, and DMF as eluents. The second dark-brown band containing the desired product was eluted with 10–20% DMF in acetone. After removal of the solvent, the dry solid was digested in 15 mL of acetonitrile and filtered. The dark-brown filtrate was reduced using a rotavap, and the residue redissolved in 10 mL of acetone. The addition of 200 mL of diethyl ether to this acetone solution precipitated the dark-orange product which was filtered and vacuum-dried. Yield: 0.20 g, 30%. Anal. Calcd. for $C_{29}H_{25}N_6Cl_2PF_6RuSO$: C, 42.35; H, 3.06; N, 10.22. Found: C, 42.62; H, 3.03; N, 10.20. 1H NMR in ppm (300 MHz, dmsO- d_6): 10.01 (d, 1H), 9.16 (d, 1H), 8.88 (d, 1H), 8.84 (d, 1H), 8.78 (d, 1H), 8.72 (d, 1H), 8.44 (t, 1H), 8.35 (t, 1H), 8.17 (t, 1H), 8.09 (t, 1H), 7.97 (dt, 2H), 7.90 (d, 1H), 7.51 (t, 1H), 7.44 (t, 1H), 7.24 (d, 1H), 7.14 (d, 1H), 6.83 (d, 1H), 5.92 (d, 1H), 3.20 (s, 3H), 2.25 (s, 3H). IR (KBr): $\nu(NCN)$, 2172; $\nu(S=O)$, 1098 cm^{-1} .

Preparation of $[Ru(bpy)_2(Cl_3pcyd)(dmsO-S)]PF_6 \cdot H_2O$. This complex was prepared by following the same procedure as above with some modification. A mixture of *cis*-Ru(bpy) $_2$ (Cl $_3$ pcyd) $_2$ (0.85 g, 1.0 mmol) and NH $_4$ PF $_6$ (0.16 g, 1.0 mmol) was refluxed in 20 mL of dmsO under argon for 30 min. The volume of the reaction solution was reduced as described above and after dissolving the residue in acetone and precipitation with diethyl ether gave 0.64 g of crude product. The pure compound was isolated by passing the crude product through the alumina column (300 g, grade V) using CH $_2$ Cl $_2$ and acetone as eluents. The second dark-brown band containing the desired product was eluted with 10% acetone in CH $_2$ Cl $_2$. After removal of the solvent, the dry solid was digested in 15 mL of acetonitrile and then filtered. The dark-brown filtrate was reduced using a rotavap, and the residue redissolved in about 10 mL of acetone. The addition of 200 mL of diethyl ether to this acetone solution precipitated the dark-orange

product which was filtered and vacuum-dried. Yield: 0.20 g, 23%. Anal. Calcd. for $C_{29}H_{26}N_6Cl_3PF_6RuSO_2$: C, 39.81; H, 2.99; N, 9.63. Found: C, 39.78; H, 2.62; N, 9.63. 1H NMR in ppm (300 MHz, dmsO- d_6): 10.00 (d, 1H), 9.17 (d, 1H), 8.87 (dd, 2H), 8.80 (d, 1H), 8.72 (d, 1H), 8.44 (t, 1H), 8.36 (t, 1H), 8.18 (t, 1H), 8.09 (t, 1H), 7.98 (dt, 2H), 7.90 (d, 1H), 7.51 (t, 1H), 7.44 (t, 1H), 7.25 (d, 1H), 7.35 (s, 1H), 6.02 (s, 1H), 3.19 (s, 3H), 2.27 (s, 3H). IR (KBr): $\nu(NCN)$ 2174; $\nu(S=O)$ 1094 cm^{-1} .

Preparation of $[Ru(bpy)_2(Cl_4pcyd)(dmsO-S)]PF_6$. A mixture of *cis*-Ru(bpy) $_2$ (Cl $_4$ pcyd) $_2$ (0.10 g, 0.11 mmol) and NH $_4$ PF $_6$ (0.018 g, 0.11 mmol) in dmsO (5 mL) was refluxed under argon for 17 min during which time the purple solution turned dark orange-yellow. After removal of dmsO at elevated temperature (~100 °C) under vacuum, the sticky solid was digested in 10 mL of acetone to which was added about 200 mL of diethyl ether, precipitating the dark-orange product which was filtered and vacuum-dried. Yield: 0.067 g, 68%. Anal. Calcd. for $C_{29}H_{23}N_6Cl_4PF_6RuSO$: C, 39.07; H, 2.60; N, 9.43. Found: C, 38.73; H, 2.31; N, 9.33. 1H NMR in ppm (300 MHz, dmsO- d_6): 10.00 (d, 1H), 9.14 (d, 1H), 8.87 (d, 1H), 8.83 (d, 1H), 8.77 (d, 1H), 8.71 (d, 1H), 8.44 (t, 1H), 8.34 (t, 1H), 8.15 (t, 1H), 8.08 (t, 1H), 8.01 (t, 1H), 7.95 (t, 1H), 7.80 (d, 1H), 7.50 (t, 1H), 7.43 (t, 1H), 7.23 (d, 1H), 7.07 (s, 1H), 3.22 (s, 3H), 2.23 (s, 3H). IR (KBr): $\nu(NCN)$, 2178; $\nu(S=O)$ 1089 cm^{-1} .

Preparation of $[Ru(bpy)_2(Cl_5pcyd)(dmsO-S)]PF_6 \cdot H_2O$. This complex was prepared by following the same procedure as above with some modification. A mixture of *cis*-Ru(bpy) $_2$ (Cl $_5$ pcyd) $_2$ (0.1 g, 0.10 mmol) and NH $_4$ PF $_6$ (0.016 g, 0.10 mmol) in dmsO (5 mL) was refluxed under argon for 12 min. The dark-orange product was isolated as above. Yield: 0.057 g, 60%. Anal. Calcd. for $C_{29}H_{24}N_6Cl_5PF_6RuSO_2$: C, 36.90; H, 2.56; N, 8.90; Cl, 18.78. Found: C, 37.09; H, 2.24; N, 8.99; Cl, 18.49. 1H NMR in ppm (300 MHz, dmsO- d_6): 9.99 (d, 1H), 9.14 (d, 1H), 8.87 (d, 1H), 8.83 (d, 1H), 8.77 (d, 1H), 8.71 (d, 1H), 8.44 (t, 1H), 8.34 (t, 1H), 8.16 (t, 1H), 8.08 (t, 1H), 8.01 (t, 1H), 7.95 (t, 1H), 7.80 (d, 1H), 7.51 (t, 1H), 7.43 (t, 1H), 7.23 (d, 1H), 3.21 (s, 3H), 2.24 (s, 3H). IR (KBr): $\nu(NCN)$, 2181; $\nu(S=O)$ 1094 cm^{-1} .

Physical Measurements. Electrochemistry. Cyclic voltammetry studies were performed using a Metrohm Autolab potentiostat/galvanostat PGSTAT30. DMF (Sigma-Aldrich, ChromosolvPlus, 99.9%, HPLC grade) was used for the studies. A three electrode arrangement consisting of a platinum disk electrode working electrode (BAS 1.6 mm diameter), a platinum wire auxiliary electrode, and a silver-wire quasi-reference electrode was used. The electrochemical cell consisted of a double jacketed glass container with an internal volume of 15 mL. Ferrocene ($E^\circ = 0.665$ V versus NHE) 8 was used as internal reference and TBAH (0.1M) was the supporting electrolyte. Argon gas was bubbled into the solutions for 10–15 min to degas them before scans were recorded.

Infrared, Electronic Absorption, and NMR Spectroscopies. Infrared spectra of S-bonded complexes in KBr mulls were obtained using a Bomem Michelson 120 FTIR spectrometer. Electronic absorption spectra were taken using a Cary 5 spectrophotometer. 1H NMR spectra were obtained at ambient temperature by using Bruker AMX-400 NMR or Bruker 300 Ultra Shield spectrometers and reference to TMS at 0.00 ppm.

Photochemistry and Quantum Yield Measurements. Photolysis experiments were performed using a 150 W xenon arc lamp (Newport model number 6255). Sample solutions in a 1.0 cm path length quartz cell were placed in a thermally jacketed sample holder at a distance of 50 cm from the light source. An infrared filter was placed in between the light source and the sample. Photoisomerism quantum yields were determined by following the method described in the literature. 4c Samples were irradiated using a Luxeon Rebel LED light source (Royal Blue, $\lambda = 447.5$ nm) mounted on 20 mm Tristar Coolbase which provided a thermal interface between the light source and D-E-700 heat sink. A Harrison 6205B Dual DC Power Supply provided operating voltage of 12 V through a Buck Puck DC driver. The DC driver is extremely dimmable and puts up to 700 mA current for LED light through a potentiometer (5 kohm). The potentiometer served to control the intensity of the LED light, and the maximum power output

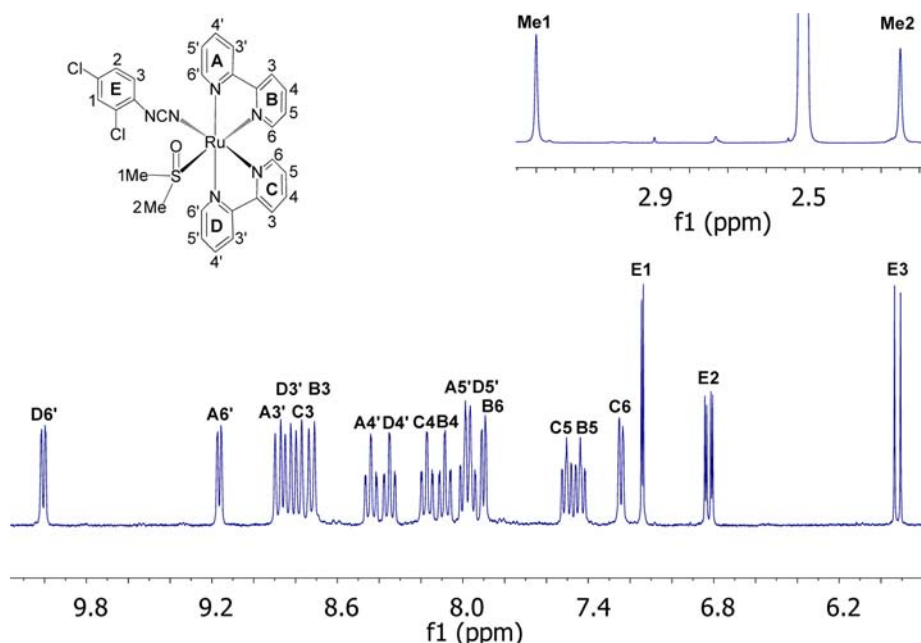


Figure 1. ^1H NMR spectrum of $[\text{Ru}(\text{bpy})_2(\text{Cl}_2\text{pcyd})(\text{dmsO-S})]^+$ in $\text{dmsO-}d_6$.

was expected to be 2520 mW. The time required to reach the maximum power output for LED is $\sim 50 \mu\text{s}$.

Elemental Analyses. All elemental analyses were performed by Canadian Microanalytical Services, Ltd. in Delta, B. C., Canada.

DFT Calculations. Hybrid HF-DFT SCF calculations of the complex's equilibrium geometry, MOs, orbital energies and spin density distributions were performed with Wave function Inc., Spartan'14 Parallel program package, using the B3LYP/6-31G* model.

RESULTS AND DISCUSSION

Synthesis. The $[\text{Ru}(\text{bpy})_2(\text{L})(\text{dmsO-S})][\text{PF}_6]$ complexes were prepared by the partial solvolysis of $[\text{Ru}(\text{bpy})_2(\text{L})_2]$ in dmsO . Some care must be taken not to heat the reagent complex too long in dmsO as both phenylcyanamide ligands can be displaced forming the known complex $[\text{Ru}(\text{bpy})_2(\text{dmsO-S})_2]^{2+}$.^{4c} A representative ^1H NMR spectrum of $[\text{Ru}(\text{bpy})_2(\text{Cl}_2\text{pcyd})(\text{dmsO-S})]^+$ is shown in Figure 1 and is consistent with *cis* coordination of phenylcyanamide and dmsO ligands which results in four inequivalent pyridine moieties. COSY analyses of this spectrum (Supporting Information, Figure S1) permitted determination of the chemical shift assignments in Figure 1. The inset to Figure 1 shows two chemical shifts belonging to the methyl groups of coordinated dmsO and is similar to those observed for sulfur bound dmsO in the structurally characterized *cis*- $[\text{Ru}(\text{bpy})_2(\text{dmsO-S})\text{Cl}]^+$.⁹ We infer that the ruthenium complexes of this study incorporate sulfur-bound dmsO .

The coordination sphere of $[\text{Ru}(\text{bpy})_2(\text{L})(\text{dmsO-S})][\text{PF}_6]$ was deliberately chosen to be similar to that of *trans*- $[\text{Ru}(\text{tpy})(\text{pic})(\text{dmsO-S})]^+$ where *pic* is 2-pyridinecarboxylate.^{5a} Both complexes possess a Ru(II) coordination sphere of four pyridine moieties, dmsO and a pseudohalide donor atom. *Trans*- $[\text{Ru}(\text{tpy})(\text{pic})(\text{dmsO-S})]^+$ undergoes photoinduced linkage isomerism forming the metastable *trans*- $[\text{Ru}(\text{tpy})(\text{pic})(\text{dmsO-O})]^+$ with $\Phi_{\text{S} \rightarrow \text{O}} = 0.25$. A slow thermal back reaction reforms *trans*- $[\text{Ru}(\text{tpy})(\text{pic})(\text{dmsO-S})]^+$ with rate $k_{\text{S} \rightarrow \text{O}} = 1 \times 10^{-3} \text{ s}^{-1}$.^{5a} Similar chemistry is expected for the $[\text{Ru}(\text{bpy})_2(\text{L})(\text{dmsO-S})]^+$ complexes and will be examined with respect to the changing electron donor properties of the phenylcyanamide ligand.

DFT Calculations. DFT calculations were performed on $[\text{Ru}(\text{bpy})_2(\text{pcyd})(\text{dmsO-S})]^+$ and $[\text{Ru}(\text{bpy})_2(\text{pcyd})(\text{dmsO-O})]^+$, and the frontier molecular orbitals and their energies of $[\text{Ru}(\text{bpy})_2(\text{pcyd})(\text{dmsO-S})]^+$ are shown in Figure 2. For those of $[\text{Ru}(\text{bpy})_2(\text{pcyd})(\text{dmsO-O})]^+$, see Supporting Information, Figure S2. The highest occupied molecular orbitals (HOMOs) of $[\text{Ru}(\text{bpy})_2(\text{pcyd})(\text{dmsO-S})]^+$ and $[\text{Ru}(\text{bpy})_2(\text{pcyd})(\text{dmsO-O})]^+$ are of mostly phenylcyanamide ligand character, and it is expected that upon oxidation considerable spin density should reside on the phenylcyanamide ligand. Indeed, Figure 3 shows

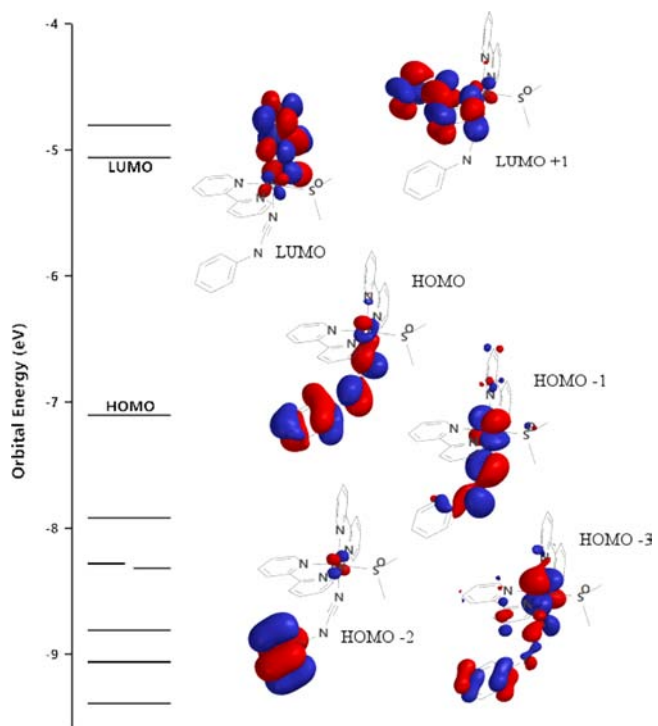


Figure 2. DFT calculation of orbital energies and selected molecular orbitals of $[\text{Ru}(\text{bpy})_2(\text{pcyd})(\text{dmsO-S})]^+$.

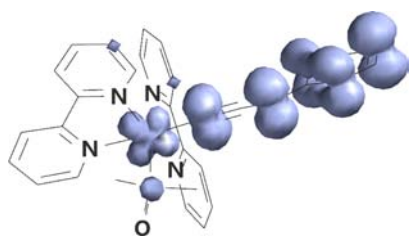


Figure 3. Spin density distribution of $[\text{Ru}(\text{bpy})_2(\text{pcyd})(\text{dmsO-S})]^{2+}$.

the spin density distribution of the oxidized complex $[\text{Ru}(\text{bpy})_2(\text{pcyd})(\text{dmsO-S})]^{2+}$ which places more than 80% of the spin on the phenylcyanamide ligand. A similar spin density distribution is seen for $[\text{Ru}(\text{bpy})_2(\text{pcyd})(\text{dmsO-O})]^{2+}$ (Supporting Information, Figure S3). Phenylcyanamide ligands are known to be noninnocent¹⁰ and because both photoinduced and thermal linkage isomerism processes depend upon the formation of the formal Ru(III) oxidation state, the donor properties of the phenylcyanamide ligand can be expected to have a significant effect on these processes.

A DFT calculation of molecular orbitals and energies was also performed on $[\text{Ru}(\text{bpy})_2(\text{Cl}_5\text{pcyd})(\text{dmsO-S})]^+$ (see Supporting Information, Figure S4). In comparison to $[\text{Ru}(\text{bpy})_2(\text{pcyd})(\text{dmsO-S})]^+$, the molecular orbitals look much the same except that those of $[\text{Ru}(\text{bpy})_2(\text{Cl}_5\text{pcyd})(\text{dmsO-S})]^+$ are generally more stable. For example, the HOMO of the Cl_5pcyd complex is 0.4 eV more stable than that of the pcyd complex, and this must be due to the electron-withdrawing properties of the chloro substituents.

Photoinduced Linkage Isomerism. Solutions of the complexes are photochromic and in ambient light readily undergo significant photoinduced linkage isomerism (Figure 4) which can be monitored by electronic absorption spectroscopy. Figure 5 shows representative visible absorption spectra resulting from blue light irradiation (450 ± 20 nm) of $[\text{Ru}(\text{bpy})_2(\text{Cl}_5\text{pcyd})(\text{dmsO-S})]^+$ to form $[\text{Ru}(\text{bpy})_2(\text{Cl}_5\text{pcyd})(\text{dmsO-O})]^+$ in dmsO. For $[\text{Ru}(\text{bpy})_2(\text{Cl}_5\text{pcyd})(\text{dmsO-S})]^+$, the dominant feature in the visible region is a MLCT transition centered at 405 nm which shifts to 512 nm with the formation of $[\text{Ru}(\text{bpy})_2(\text{Cl}_5\text{pcyd})(\text{dmsO-O})]^+$. The metastable $[\text{Ru}(\text{bpy})_2(\text{L})(\text{dmsO-O})]^+$ complexes slowly revert back to $[\text{Ru}(\text{bpy})_2(\text{L})(\text{dmsO-S})]^+$ with first-order rate $k_{\text{O,S1}}$. These were determined for each complex and placed in Table 1 together with the electronic absorption data of $[\text{Ru}(\text{bpy})_2(\text{L})(\text{dmsO-O})]^+$ and $[\text{Ru}(\text{bpy})_2(\text{L})(\text{dmsO-S})]^+$ complexes. Quantum yields for the photoinduced linkage isomerism $\Phi_{\text{S} \rightarrow \text{O}}$ were also determined and have been placed in Table 1.

As shown by transient absorption spectroscopy,⁵ excited state Ru–S to Ru–O rearrangement is an intramolecular process. At longer reaction times, the more labile Ru–O isomer can

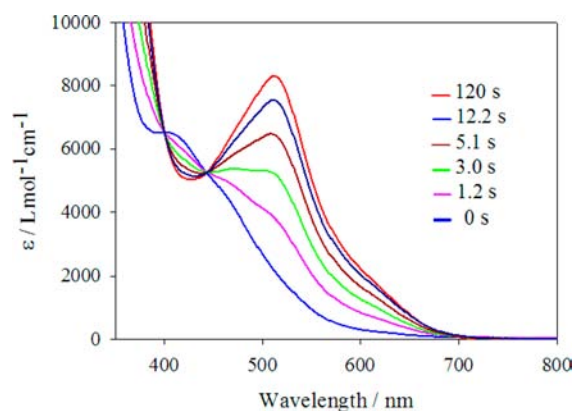


Figure 5. Visible light irradiation of $[\text{Ru}(\text{bpy})_2(\text{Cl}_5\text{pcyd})(\text{dmsO-S})]^+$ (blue line) forming its linkage isomer $[\text{Ru}(\text{bpy})_2(\text{Cl}_5\text{pcyd})(\text{dmsO-O})]^+$ (red line) in dmsO. Irradiation times in legend.

undergo ligand substitution which is why reversibility can be lost in strong donor solvents. In dmsO solution, the only way that this would influence the quantum yield would be if ligand substitution caused the reformation of the Ru–S isomer. However, the thermal rates of linkage isomerism $k_{\text{O,S1}}$ in Table 1 are slow, and measurement of the quantum yield at different irradiation times show no significant difference in results.

In past studies, the quantum yield of isomerization $\Phi_{\text{S} \rightarrow \text{O}}$ was shown to vary considerably depending on the nature of the ancillary ligands. For example, $[\text{Ru}(\text{tpy})(\text{L}_2)(\text{dmsO-S})]^{n+}$, where L_2 is acetylacetonate, tetramethylethylene diamine, 2,2'-bipyridine, 2-pyridinecarboxylate, and 4-methyl-2-pyridinecarboxylate, has $\Phi_{\text{S} \rightarrow \text{O}} = <10^{-4}$, 0.007, 0.024, 0.25, and 0.79, respectively.⁴¹ In these complexes, the electronic properties of L_2 vary considerably, and it is difficult to deconvolute a specific property responsible for the change in $\Phi_{\text{S} \rightarrow \text{O}}$ with bidentate ligand. A DFT study of these complexes^{4m} indicated that the percentage ruthenium character of the HOMO followed the trend in quantum yields of isomerization, being greatest for the largest quantum yield. The authors concluded that as the excited state responsible for linkage isomerism is ³MLCT, the Ru(III) character of the state must be important. This result cannot be directly compared to the complexes of this study because the HOMO is mostly of phenylcyanamide character (Figure 2). Nevertheless, in Table 1, there is a clear trend in the quantum yield of photoinduced linkage isomerism, decreasing as the number of chloro-substituents of the phenylcyanamide ligand decrease. This trend is opposite to that of the thermal back reaction $k_{\text{O,S1}}$ but likely has the same chemical explanation, the relative electron donor properties of phenylcyanamide ligands. Assuming analogous photochemistry to that of $[\text{Ru}(\text{tpy})(\text{pic})(\text{dmsO-S})]^+$,^{5a} the magnitude of $\Phi_{\text{S} \rightarrow \text{O}}$ is deter-

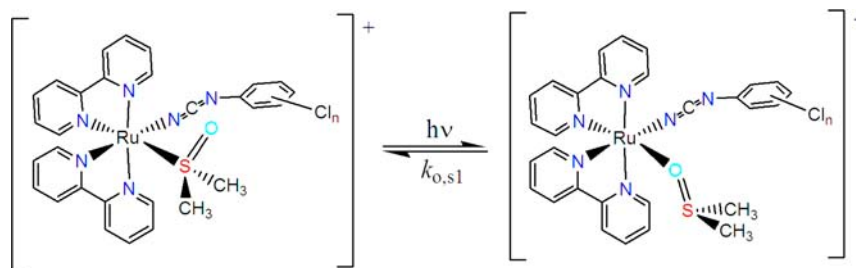


Figure 4. Photoinduced linkage isomerism and thermal rate of linkage isomerism of $[\text{Ru}(\text{bpy})_2(\text{L})(\text{dmsO-S})]^+$ complexes.

Table 1. Spectroscopic Data,^a Linkage Isomerism Quantum Yields,^b and Linkage Isomerism Rates^c of [Ru(bpy)₂(L)(dmsO)][PF₆] Complexes

L ⁻	Ru-(dmsO-S) isomer	Ru-(dmsO-O) isomer	Φ _{S→O} ^b	k _{o,s1} ^c (10 ⁻³ s ⁻¹)
Cl ₃ pcyd ⁻	294 (61200), 405 (6500), 470 (sh, 4100)	512 (8300)	0.43	2.61
Cl ₄ pcyd ⁻	296 (59900), 409 (6100), 465 (sh, 4400)	506 (8000)	0.34	2.31
Cl ₃ pcyd ⁻	293 (62000), 405 (6200), 515 (sh, 2900)	506 (6900)	0.28	2.41
Cl ₂ pcyd ⁻	288 (49500), 405 (5600), 470 (sh, 3400)	513 (5900)	0.12	2.84
Clpcyd	287 (65900), 409 (5700), 468 (sh, 3800)	505 (4300)	0.11	4.30
pcyd ⁻	284 (50500), 400 (5200), 470 (sh, 3700)	517 (3700)	0.06	4.50

^aλ_{max} (ε)/nm (M⁻¹ cm⁻¹), sh = shoulder, in dmsO. ^bQuantum yields measured following the procedure described in ref 4e. ^ck_{o,s1} obtained by irradiating the Ru-S complex and measuring the first-order decay of the Ru-O complex in dmsO.

mined by a linkage isomerism rate from the ³MLCT excited state of [Ru(bpy)₂(L)(dmsO-S)]^{+*} to [Ru(bpy)₂(L)(dmsO-O)]^{+*} that is significantly greater than the rate of ³MLCT decay to the ground state of [Ru(bpy)₂(L)(dmsO-S)]⁺. If the rate of ³MLCT decay is constant for the complexes in Table 1,¹¹ the decrease in Φ_{S,O} with the phenylcyanamide donor properties must be due to an increase in the activation barrier to excited state linkage isomerism. It is likely that the donor properties of the phenylcyanamide ligand stabilize the Ru-S isomer and thereby inhibit rearrangement to the Ru-O isomer in the ³MLCT state.

Cyclic Voltammetry. As discussed in the introduction, the Ru-O isomer is preferred in the Ru(III) oxidation state. For example, upon oxidation of [Ru(tpy)(pic)(dmsO-S)]⁺ at 1.61 V vs NHE forming the Ru(III) ion, the growth of a new wave at 0.86 V vs NHE is observed due to formation of the Ru-O species.^{4f} In contrast, the cyclic voltammograms of [Ru(bpy)₂(L)(dmsO-S)]⁺ complexes in dmsO show only a single reversible oxidation wave with repeated scans. This is illustrated by the representative voltammogram of [Ru(bpy)₂(Cl₃pcyd)(dmsO-S)]⁺ in Figure 6 (blue line) which shows only a single

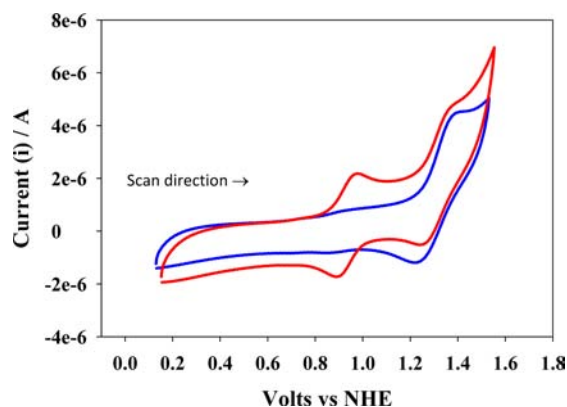


Figure 6. Cyclic voltammograms of [Ru(bpy)₂(Cl₃pcyd){dmsO(-S)}]⁺ (blue) and after partial photolysis (red), in dmsO and 0.1 M TBAH, 1.0 V/s.

reversible wave at 1.29 V vs NHE. The lack of evidence for linkage isomerism with oxidation strongly suggests that the Ru(III) ion is not formed and indeed the DFT analysis of [Ru(bpy)₂(Cl₃pcyd)(dmsO-S)]²⁺ (Figure 3) supports a formal assignment to the phenylcyanamide ligand couple L(0/-). Partial photolysis of this solution generates some [Ru(bpy)₂(Cl₃pcyd)(dmsO-O)]⁺ species and results in the growth of a new wave at more negative potential which again based on DFT analysis of [Ru(bpy)₂(Cl₃pcyd)(dmsO-O)]²⁺ (see Sup-

porting Information, Figure S3), we assign to the L(0/-) couple.

To observe the Ru(III/II) couple of the Ru-S species, acetonitrile solutions of [Ru(bpy)₂(L)(dmsO-S)]⁺ were investigated, and these showed a dramatic scan rate dependence of their cyclic voltammetry (Figure 7 and Table 2). In Figure 7,

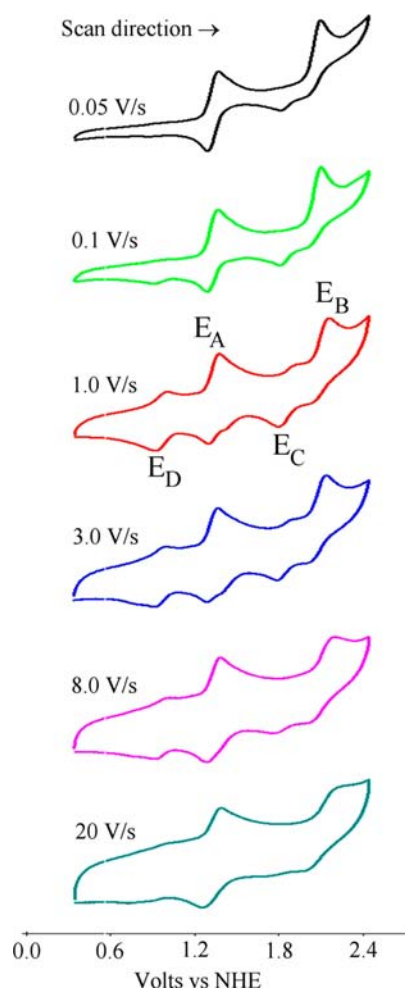


Figure 7. Cyclic voltammograms of [Ru(bpy)₂(Cl₃pcyd)(dmsO-S)]⁺ in acetonitrile, 0.1 M TBAH, at scan rates from 0.05 to 20 V/s.

the cyclic voltammogram of [Ru(bpy)₂(Cl₃pcyd)(dmsO-S)]⁺ at a scan rate of 0.05 V/s shows that an anodic wave at 1.35 V, belonging to the L(0/-) couple (E_A), is followed by an anodic wave at 2.15 V, which we assign to an irreversible Ru(III/II) couple (E_B). However, this irreversible Ru(III/II) couple must be followed by a process (the cathodic wave at 1.79 V) which

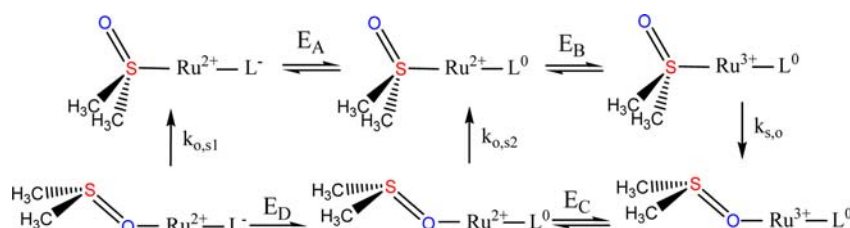
Table 2. Cyclic Voltammetry Data^a of [Ru(bpy)₂(L)(dmsO)][PF₆] Complexes in Acetonitrile

L ⁻	Ru-(dmsO-S) isomer		Ru-(dmsO-O) isomer	
	E _A (V)	E _B (V)	E _C (V)	E _D (V)
Cl ₅ pcyd ⁻	1.31	2.09	1.79	0.95
Cl ₄ pcyd ⁻	1.30	2.22 ^b		
Cl ₃ pcyd ⁻	1.24	2.02	1.69	0.95
Cl ₂ pcyd ⁻	1.15	1.93	1.71	0.90
Clpcyd ⁻	1.04 ^c			
pcyd ⁻	1.01 ^b			

^aIn acetonitrile, scan rate 1.0 V/s, 0.1 M tetrabutylammonium hexafluorophosphate, V vs NHE. ^bIrreversible, anodic peak potential. ^cPartially reversible.

recovers the complex to achieve a cathodic peak current which matches the anodic peak current of the L(0/-) couple (E_A). When the scan rate is increased from 0.1 to 3 V/s, the growth of two new couples (E_C and E_D) is observed. If the rate is increased to the limit of our instrumentation, these couples lose current intensity, and the complex's cyclic voltammetry is simplified to L(0/-) and Ru(III/II) couples or E_A and E_B, respectively.¹²

The scan rate dependent voltammograms in Figure 7 can be interpreted by redox-induced linkage isomerism as shown in Scheme 1. At a scan rate of 0.05 V/s to positive potential, oxidation (E_A) of (dmsO-S)-Ru²⁺-L⁻ forms (dmsO-S)-Ru²⁺-L⁰. At higher positive potential E_B, the (dmsO-S)-Ru³⁺-L⁰ species forms and undergoes a relatively fast rate of linkage isomerism *k*_{s,o} forming (dmsO-O)-Ru³⁺-L⁰. Scanning to negative potential, this species undergoes reduction (E_C) to form (dmsO-O)-Ru²⁺-L⁰ and then rearranges with rate *k*_{s,o2} forming (dmsO-S)-Ru²⁺-L⁰ which is then reduced (E_A), yielding the initial complex. At scan rates comparable or higher than *k*_{s,o2}, the (dmsO-O)-Ru²⁺-L⁰ species can be reduced (E_D) before rearrangement can occur, forming (dmsO-O)-Ru²⁺-L⁻ which then undergoes rearrangement *k*_{s,o1}. In this case, a steady state concentration of Ru-O species is maintained, and all the redox couples of Scheme 1 are observed (see Figure 5, scan rate 1.0 V/s). Finally, if the scan rate is much faster than the linkage isomerism rate *k*_{s,o}, no Ru-O species will be generated, and the cyclic voltammogram (Figure 7, 20 V/s) is that of Ru-S species (E_A and E_B). From the scan rate dependent cyclic voltammograms, it is possible to estimate the linkage isomerism rates of *k*_{s,o} ≈ 50 s⁻¹ and *k*_{s,o2} ≈ 0.2 s⁻¹. These rates are expected to vary only slightly for the other complexes of this study based on the slight variation of *k*_{s,o1} with phenylcyanamide ligand in Table 1. As seen by the electrochemical data in Table 2, the L = Cl₂pcyd⁻, Cl₃pcyd⁻, and Cl₅pcyd⁻ complexes are described by Scheme 1 while the other complexes showed poor reversibility of the L⁰/L⁻ or Ru(III/II) couples.

Scheme 1. Assignment of the Redox Couples and Rates of Linkage Isomerism**CONCLUSION**

Six new complexes [Ru(bpy)₂(L)(dmsO-S)]⁺, where L⁻ is Cl₅pcyd⁻, Cl₄pcyd⁻, Cl₃pcyd⁻, Cl₂pcyd⁻, Clpcyd⁻, and pcyd⁻, have been synthesized and characterized by ¹H NMR and electronic absorption spectroscopy and cyclic voltammetry. These complexes readily undergo photoinduced linkage isomerism to metastable [Ru(bpy)₂(L)(dmsO-O)]⁺ followed by a relatively slow thermal rearrangement back to [Ru(bpy)₂(L)(dmsO-S)]⁺. The trend in quantum yields suggests that the rate of linkage isomerism in the ³MLCT excited state is controlled by the donor properties of the phenylcyanamide ligand. DFT calculations of both [Ru(bpy)₂(pcyd)(dmsO-S)]⁺ and [Ru(bpy)₂(pcyd)(dmsO-O)]⁺ show a mostly phenylcyanamide HOMO, and the oxidized complexes show a spin density distribution mostly localized on the phenylcyanamide ligand. The cyclic voltammetry of these complexes showed two oxidation processes: a phenylcyanamide L(0/-) couple followed by a Ru(III/II) couple at more positive potential. Upon oxidation to Ru(III), the complexes rearranged to form Ru-O linkage isomers, and the scan rate dependent voltammograms permitted estimates of the rates of linkage isomerism.

Future studies will use photoinduced linkage isomerism to alter the mixed-valence properties of dinuclear complexes that incorporate phenylcyanamide bridging ligands.

ASSOCIATED CONTENT**Supporting Information**

A COSY spectrum of [Ru(bpy)₂(Cl₂pcyd)(dmsO-S)]⁺, DFT calculated orbital energies and MOs of [Ru(bpy)₂(pcyd)(dmsO-O)]⁺, spin density distribution of [Ru(bpy)₂(pcyd)(dmsO-O)]²⁺, and DFT calculated orbital energies and MOs of [Ru(bpy)₂(Cl₃pcyd)(dmsO-S)]⁺. This material is available free of charge via the Internet at <http://pubs.acs.org>.

AUTHOR INFORMATION**Corresponding Author**

*E-mail: robert_crutchley@carleton.ca.

Notes

The authors declare no competing financial interest.

ACKNOWLEDGMENTS

This work is supported by Carleton University and the Natural Sciences and Engineering Research Council of Canada.

REFERENCES

- (1) (a) Mustroph, H.; Stollenwerk, M.; Bressau, V. *Angew. Chem., Int. Ed.* **2006**, *45*, 2016–2035. (b) Dong, H.; Zhu, H.; Meng, Q.; Gong, X.; Hu, W. *Chem. Soc. Rev.* **2012**, *41*, 1754–1808.
- (2) (a) Zhang, J.; Zou, Q.; Tian, H. *Adv. Mater.* **2013**, *25*, 378–399. (b) Bleger, D.; Yu, Z.; Hecht, S. *Chem. Commun.* **2011**, *47*, 12260–

12266. (c) Russew, M.-M.; Hecht, S. *Adv. Mater.* **2010**, *22*, 3348–3360.

(3) Rack, J. J.; Winkler, J. R.; Gray, H. B. *J. Am. Chem. Soc.* **2001**, *123*, 2432–2433.

(4) (a) Sano, M.; Taube, H. *Inorg. Chem.* **1994**, *33*, 705–709. (b) Tomita, A.; Sano, M. *Inorg. Chem.* **1994**, *32*, 5825–5830. (c) Smith, M. K.; Gibson, J. A.; Young, C. G.; Broomhead, J. A.; Junk, P. C.; Keene, F. R. *Eur. J. Inorg. Chem.* **2000**, 1365–1370. (d) Rack, J. J.; Mockus, N. V. *Inorg. Chem.* **2003**, *42*, 5792–4. (e) Mockus, N.; Petersen, J. L.; Rack, J. J. *Inorg. Chem.* **2006**, *45*, 8–10. (f) Rachford, A. A.; Petersen, J. L.; Rack, J. J. *Inorg. Chem.* **2005**, *44*, 8065–8075. (g) Butcher, D. P.; Rachford, A. A.; Petersen, J. L.; Rack, J. J. *Inorg. Chem.* **2006**, *45*, 9178–9180. (h) Rachford, A. A.; Petersen, J. L.; Rack, J. J. *Dalton Trans.* **2007**, 3245–3251. (i) Mockus, N.; Marquad, S.; Rack, J. J. *J. Photochem. Photobiol. A* **2008**, *200*, 39–43. (j) McClure, B. A.; Abrams, E. R.; Rack, J. J. *J. Am. Chem. Soc.* **2010**, *132*, 5428–5436. (k) McClure, B. A.; Mockus, N. V.; Butcher, D. P.; Lutterman, D. A.; Turro, C.; Petersen, J. L.; Rack, J. J. *Inorg. Chem.* **2009**, *48*, 8084–8091. (l) Rack, J. J. *Coord. Chem. Rev.* **2009**, *253*, 78–85. (m) Lutterman, D. A.; Rachford, A. A.; Rack, J. J.; Turro, C. *J. Phys. Chem. A* **2009**, *113*, 11002–11006. (n) McClure, B. A.; Rack, J. J. *Angew. Chem., Int. Ed.* **2009**, *48*, 8556–8558. (o) Mockus, N. V.; Rabinovich, D.; Petersen, J. L.; Rack, J. J. *Angew. Chem., Int. Ed.* **2008**, *47*, 1458–1461. (p) Lutterman, D. A.; Rachford, A. A.; Rack, J. J.; Turro, C. *J. Phys. Chem. Lett.* **2010**, *1*, 3371–3375. (q) Porter, B. L.; McClure, B. A.; Abrams, E. R.; Engle, J. T.; Ziegler, C. J.; Rack, J. J. *J. Photochem. Photobiol. A* **2011**, *217*, 341–346. (r) King, A. W.; Jin, Y.; Engle, J. T.; Ziegler, C. J.; Rack, J. J. *Inorg. Chem.* **2013**, *52*, 2086–2093.

(5) (a) Rachford, A. A.; Rack, J. J. *J. Am. Chem. Soc.* **2006**, *128*, 14318–14324. (b) McClure, B. A.; Rack, J. J. *Inorg. Chem.* **2011**, *50*, 7586–7590.

(6) Evans, C. E. B.; Naklicki, M.; Rezvani, A.; White, C.; Veniamin, V.; Crutchley, R. J. *J. Am. Chem. Soc.* **1998**, *120*, 13096–13103.

(7) Rezvani, A. R.; Crutchley, R. J. *Inorg. Chem.* **1994**, *33*, 170–174.

(8) Gennett, T.; Milner, D. F.; Weaver, M. J. *J. Phys. Chem.* **1985**, *89*, 2787–2794.

(9) (a) Heseck, D.; Inoue, Y.; Everitte, S. R. L.; Ishida, H.; Kunieda, M.; Drew, M. G. B. *J. Chem. Soc., Dalton Trans.* **1999**, 3701–3709. (b) Wang, Y.; Eichhorn, D. M.; Goswami, N.; Zhao, Q.; Rillema, D. P. *J. Chem. Crys.* **1999**, *29*, 277–281.

(10) Carmen, H.; Kravtsov, P.; Choudhuri, M.; Sirianni, E. R.; Yap, G. P. A.; Lever, A. B. P.; Crutchley, R. J. *Inorg. Chem.* **2013**, *52*, 1621–1630.

(11) For the $[\text{Ru}(\text{bpy})_2(\text{L})(\text{dmsO-S})]^+$ complexes in Table 1, the wavelength of the MLCT transition at approximately 400 nm does not vary significantly and indicates that the energy gap between ground and $^1\text{MLCT}$ excited state is unchanged. It is reasonable to suggest that the energy gap between $^3\text{MLCT}$ and ground state is also unchanged and because of this the rate of nonradiative decay will remain constant.

(12) The small cathodic wave near 1.35 V is probably not a decomposition impurity as it is not present at a scan rate of 0.05 V/s. It is also not observed at a scan rate of 20 V/s and so it may be a Ru-O species. We suggest that after reduction (E_c) some of the Ru-O species may be adsorbed onto the surface of the working electrode and that this is the species responsible for the cathodic wave near 1.35 V.